http://dx.doi.org/10.1109/NANOTECH.2018.8653560

The Resistivity Size Effect in Epitaxial Ru(0001) and Co(0001) Layers

Erik Milosevic*, Sit Kerdsongpanya, Daniel Gall
Department of Materials Science and Engineering
Rensselaer Polytechnic Institute
110 8th St, Troy, NY 12180
*milose@rpi.edu

***Abstract*— Ru(0001) and Co(0001) films with thickness *d* ranging from 5 to 300 nm are sputter deposited onto Al_2O_3(0001) substrates in order to quantify and compare the resistivity size effect. Both metals form epitaxial single crystal layers with their basal planes parallel to the substrate surface and exhibit a root-mean-square roughness < 0.4 nm for Ru and < 0.9 nm for Co. Transport measurements on these layers have negligible resistance contributions from roughness and grain boundary scattering which allows direct quantification of electron surface scattering. The measured resistivity ρ vs *d* is well described by the classical Fuchs-Sondheimer model, indicating a mean free path for transport within the basal plane of $\lambda = 6.7 \pm 0.3$ nm for Ru and $\lambda = 19.5 \pm 1.0$ nm for Co. Bulk Ru is 36% more resistive than Co; in contrast, Ru(0001) layers with $d \leq 25$ nm are more conductive than Co(0001) layers, which is attributed to the shorter λ for Ru. The determined λ-values are utilized in combination with the Fuchs-Sondheimer and Mayadas-Shatzkes models to predict and compare the resistance of polycrystalline interconnect lines, assuming a grain boundary reflection coefficient $R = 0.4$ and accounting for the thinner barrier/adhesion layers available to Ru and Co metallizations. This results in predicted 10 nm half-pitch line resistances for Ru, Co, and Cu of 1.0, 2.2, and 2.1 kΩ/µm, respectively.**

Keywords—Interconnects, Ruthenium, Cobalt, BEOL, MOL, Resistivity Scaling, Mean Free Path, Alternative Metals

I. Introduction

Continued advancements in integrated circuit technology has led to a reduction in the interconnect half-pitch below the mean free path of the line metal, causing a dramatic increase in the resistivity [1] which is attributed to electron scattering at surfaces [2–5], grain boundaries [6–11], and surface roughness [12–15]. This increase in resistivity ρ is a major challenge for the semiconductor industry, resulting in many recent research efforts that focus on improving current metallization schemes [4,5,7,16,17] as well as on exploring potential replacement materials for copper [18–26]. Of the many potential replacement materials under investigation, Ru and Co attract particular attention due to their many benefits over traditional Cu and W metallizations, including: (1) lower predicted size effect scaling [27] (2) lower thermal budgets, as compared to W, allowing defect healing and grain growth at feasible annealing temperatures [20], (3) larger electromigration resistance, as compared to Cu, and (4) thinner barrier/adhesion layers [22,28], allowing for greater metal fill areas in trenches and lower via resistances between levels [29]. In fact, the via resistance and electromigration benefits of Co are sufficient to justify its use in current Intel chips [30].

In this article, we directly compare the resistivity scaling of Ru and Co in confined dimensions using transport measurements on high quality epitaxial films as well as discussing their potential performance in polycrystalline line structures. The use of single crystal epitaxial layers to quantify resistivity scaling has the advantage of removing the confounding effects from electron-grain boundary scattering, allowing direct quantification of resistance due to surface scattering and a more confident determination of key conduction parameters, with the most important being the electron-phonon mean free path λ. This is done by fitting measured resistivity vs thickness *d* data with the classical Fuchs-Sondheimer model [31,32], yielding $\lambda = 6.7 \pm 0.3$ and 19.5 ± 1.0 nm for Ru and Co, respectively, as well as a clear resistivity cross-over at $d = 25$ nm, below which Ru conduction exceeds that of Co. In addition, we use the measured λ and a combination of the approximate Fuchs-Sondheimer (FS) [31,32] and Mayadas-Shatzkes (MS) [33] models [2] to predict and compare the resistivities and resulting resistances of polycrystalline interconnect lines of Ru, Co and Cu for the case of a 2:1 aspect ratio trench, including appropriate adhesion/barrier thicknesses for each metallization scheme. The results of these calculations indicate that Ru will exceed Cu conductance for wire widths $w < 19$ nm and that Co conductance becomes comparable to that of Cu at $w = 10$ nm.

II. Experimental Details

All films were deposited onto degassed 1×1 cm polished Al_2O_3(0001) substrates in a three chamber ultra-high vacuum DC magnetron sputter deposition system with a base pressure below 10^{-9} torr. Films were deposited using a power of 60 and 50 W to the Ru and Co targets, respectively, in 3.0 mTorr 99.999% Ar and with substrate temperatures of 350 °C for Ru, and 300 °C for Co. *In situ* annealing was used to further improve the crystalline quality. Ru films were annealed using a temperature ramp up to 1000 °C for a total of 3 hours, and Co films were annealed at 500 °C for one hour. The deposition time was adjusted to vary the layer thickness $d = 5$-80 nm for Ru and $d = 7$-300 nm for Co. Electrical transport

NSF Nos. 1740271 and 1712752, NYSTAR C150117.

measurements were taken using a linear four-point probe with a 1 mm interprobe spacing and a current of 1-100 mA. Film thickness and roughness values were determined from X-ray reflectivity (XRR) analyses. The crystalline quality and epitaxial relationships were determined from x-ray diffraction analyses, using a Panalytical X'pert PRO MPD system with a hybrid mirror with a Ge(220) two bounce monochromator, and a PW3018/00 PIXcel line detector operated in scanning mode.

III. Film Structure

Figure 1 shows overlaid representative x-ray diffraction results from a nominally 80-nm-thick Ru(0001) layer and a nominally 40-nm-thick Co(0001) layer, both deposited on $Al_2O_3(0001)$ substrates. The diffractograms in the figure are sections of θ-2θ scans, plotted from 41.0° to 45.5°. They show peaks at 41.685°, 42.17°, and 44.54° which are attributed to the sapphire 0006, Ru 0002, and Co 0002 reflections, respectively. These peak positions indicate a negligible (< 0.01%) strain in the film normal direction for Ru, and a slight (-0.10%) compressive strain in the film growth direction for Co, indicating in-plane biaxial tensile strain which may be attributed to the 9.4% lattice mismatch between the c-plane sapphire surface and the Co basal plane [34] and/or the relatively large difference in thermal expansion coefficients between the layer and the substrate [35,36].

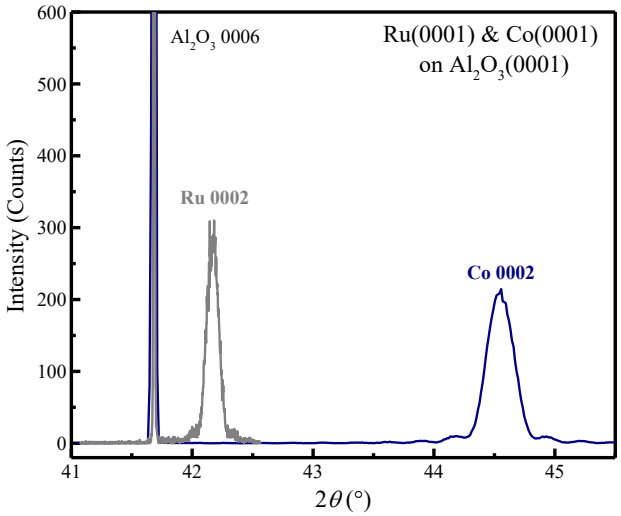

Fig. 1. Overlaid representative θ-2θ diffractograms for epitaxial $Ru(0001)/Al_2O_3(0001)$ with thickness d = 77.8 nm (gray) and epitaxial $Co(0001)/Al_2O_3(0001)$ with thickness d = 36.1 nm (blue).

Both patterns exhibit periodic fringes (more clearly visible for Co) that flank the Ru and Co 0002 peaks and are attributed to Laue oscillations that result from the interference between the upper and lower metal film surfaces and indicate a low roughness [37]. This is consistent with XRR analyses, which show that the Ru and Co layers exhibit smooth surfaces with root-mean-square roughnesses < 0.4 nm and < 0.9 nm for all thicknesses, respectively. Further diffraction analyses (not shown for brevity) but similar to those presented in [38] and [39] reveal that all films are mono-crystalline and exhibit an epitaxial layer-substrate relationship of $\text{metal}[0001] \| Al_2O_3[0001]$ and $\text{metal}[10\bar{1}0] \| Al_2O_3[11\bar{2}0]$ for both Ru and Co. This is verified using ω-rocking curves that show the alignment along the growth direction, and φ-scans from asymmetric reflections that show in-plane orientation. In addition, no misoriented grains were detected in θ-2θ scans acquired in powder diffraction mode over a large 2θ range from 5° to 90°.

IV. Elecrical Transport

Figure 2 shows the measured Ru(0001) and Co(0001) room-temperature resistivity ρ plotted as a function of film thickness d. The Ru layer with largest thickness d = 77.8 nm has a resistivity of ρ = 7.73 ± 0.15 μΩcm, which is close to the reported bulk Ru basal plane resistivity of 7.6 μΩcm [40], indicating negligible contribution from surface scattering. The resistivity increases with decreasing Ru thickness to ρ = 12.58 ± 0.25 μΩcm for d = 5.3 nm. The thickest Co film with d = 293 nm exhibits a ρ = 6.35 ± 0.21 μΩcm, which is close to ρ = 6.50 ± 0.22 μΩcm measured for d = 194 nm, indicating that surface scattering contributes negligibly to the measured resistivity for the thickest Co films. We note, however, that this resistivity is 13-15% larger than the reported value for the Co basal plane [41], which we attribute to residual defects and impurities in our Co films. The Co resistivity increases to ρ = 15.17 ± 0.64 μΩcm for d = 6.9 nm. For both metals, the observed increase in ρ with decreasing d is attributed solely to the effect of electron-surface scattering, since grain boundary scattering is absent in these epitaxial mono-crystalline films. Further we note that the effect of surface roughness on the resistivity in these layers is expected to be negligible (< 1% correction), based on the roughness measured by XRR and estimating the impact on the resistivity using both Namba's classical model [12] and Zhou's step-reflection model [15].

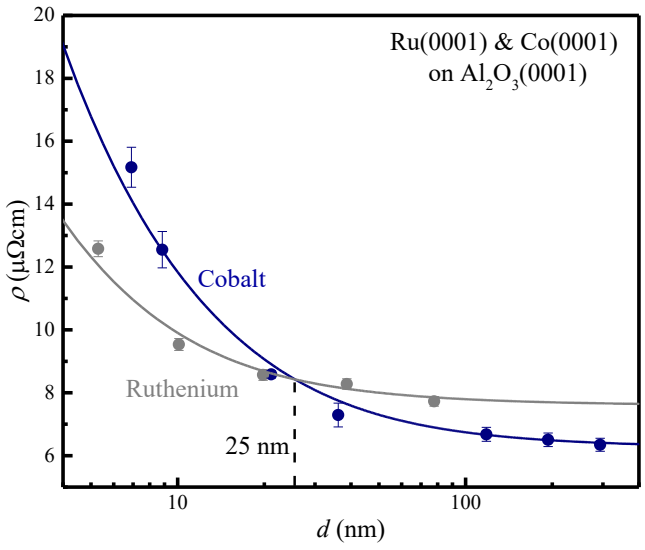

Fig. 2. Resistivity ρ of epitaxial Ru(0001) (gray) and Co(0001) (blue) layers vs film thickness d. The lines indicate the result from curve fitting using the Fuchs-Sondheimer model.

The solid lines in Fig. 2 are the result of curve fitting using the integral form of the Fuchs-Sondheimer (FS) model [2,31,32]. This is done by assuming completely diffuse surface scattering at both the top surface and the substrate-layer

interface, i.e. $p_1 = p_2 = 0$. The fitting yields mean free paths for conduction in the basal plane of $\lambda = 6.7 \pm 0.3$ nm for Ru(0001) and $\lambda = 19.5 \pm 1.0$ nm for Co(0001). The value for Ru is in good agreement with the previous theoretical prediction of $\lambda = 6.76$ nm [26,27]. In contrast, our λ for Co is 49% larger than the predicted 13.1 nm [27]. We attribute this discrepancy to the limited validity of the FS model, which is based on a purely classical electron transport description. Thus, both the data fitting in Fig. 2 as well as the theoretical prediction in [27] are limited by the accuracy of classical transport, which tends to deviate from the quantum mechanical description with decreasing feature size [1,8,42–45].

The data in Fig. 2 shows that Co has a more pronounced resistivity size effect than Ru. For example, the Ru resistivity increases from $\rho = 8.28 \pm 0.17$ to 8.57 ± 0.17 μΩcm for $d = 38.7$ to 19.8 nm, while the increase for Co over a similar thickness range, $d = 36.1$ - 21.1 nm, is 4.5 times stronger, with $\rho = 7.29 \pm 0.38$ and 8.58 ± 0.44 μΩcm, respectively. This results in a clear resistivity crossover at a layer thickness of 25 nm. That is, Co(0001) is more conductive than Ru(0001) for layers with $d > 25$ nm, but Ru(0001) is more conductive than Co(0001) for $d < 25$ nm. This is because Co has a smaller bulk resistivity ρ_o while Ru has a smaller product $\rho_o\lambda$ with this latter factor defining the resistivity in the limit of narrow wires within the classical or semiclassical transport models (including FS) [26,27,46]. We note that the resistivity crossover at 25 nm is for the case of single-crystal thin films, while the crossover is expected at larger critical dimensions for both interconnect lines and polycrystalline microstructures, due to additional electron scattering at side walls and grain boundaries, respectively, as discussed in the following.

The resistance of Ru and Co interconnect lines is directly affected by the quantified resistivity scaling. Thus, in the following, we use the measured λ values and the approximate forms of the FS and MS models to estimate the resistivity scaling for narrow interconnect lines. We assume a 2:1 aspect ratio trench, a variable half-pitch width w, a barrier/adhesion/liner layer at the bottom and sidewalls with a thickness t, and a width-dependent grain size in the transport direction of $2w$-t, as illustrated in Fig. 3(a). We neglect the effects of line-edge roughness and conduction contributions from the barrier/adhesion layers, despite that these may be considerable effects [47,48], and employ the classical transport models despite their limitations for narrow lines. Nevertheless, we believe that this method provides a fair and direct quantitative comparison of the conductance of Ru, Co, and Cu lines. We use the reported bulk resistivities $\rho_o = 7.6$, 5.6, and 1.7 μΩcm for Ru [40], Co [41], and Cu [2], respectively, where the Ru and Co values are for conduction in the basal plane. The mean free path $\lambda = 6.7 \pm 0.3$ and 19.5 ± 1.0 nm for Ru and Co are taken from our experiments, and $\lambda = 39$ nm for Cu from previous reports [49]. Electron scattering is assumed to be completely diffuse for all surfaces [4,5,26,50–52], and the grain boundary reflection coefficient is set to $R = 0.4$ for all three metals. While it is expected that these three metals likely exhibit different R values [53], the reported values range from $R = 0.3$ to 0.99 for Ru [24,54,55], from 0.07 to 0.6 for Co [52,56–58], and from 0.25 to 0.45 for Cu [1,2,59–64]. Thus, due to these large and overlapping ranges, we believe

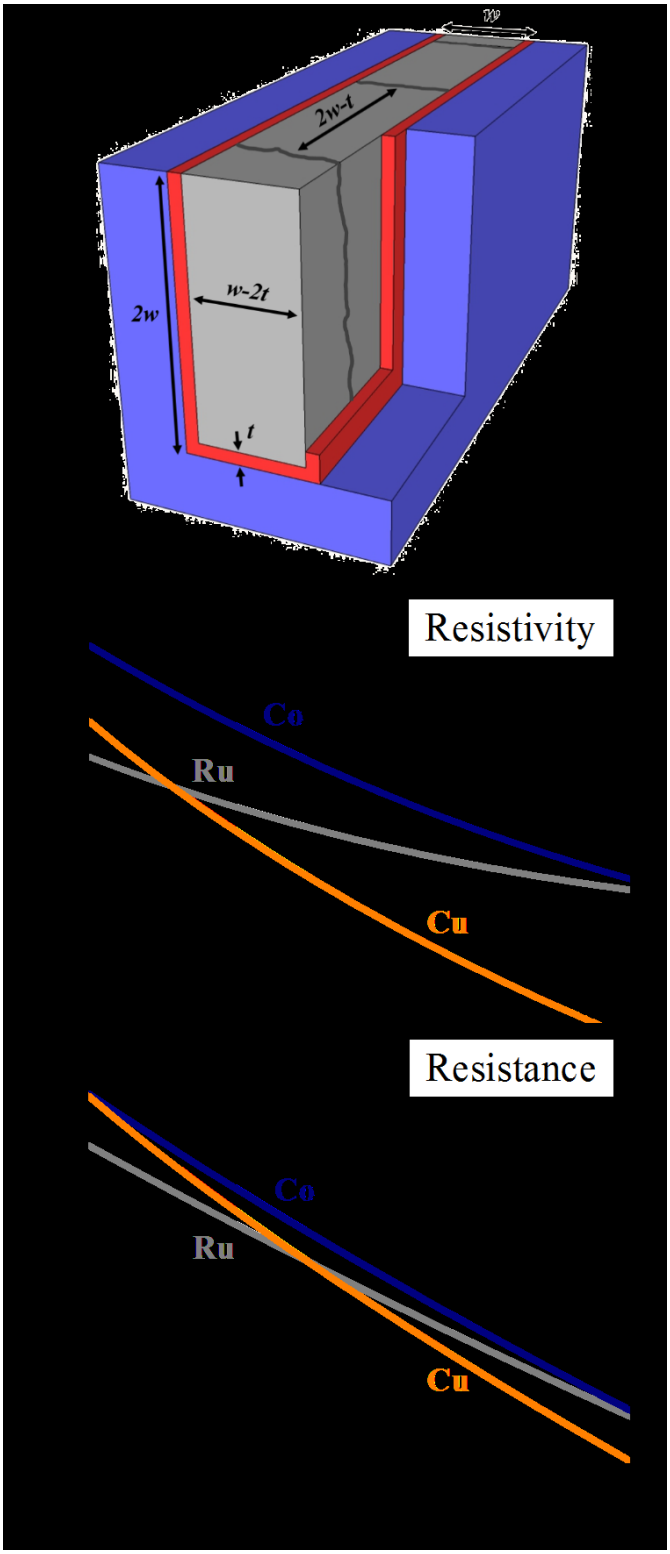

Fig. 3. (a) Schematic of a 2:1 aspect ratio interconnect line with a half-pitch w, a liner thickness t, and a $2w$-t grain size along the growth direction. Predicted (b) resistivity and (c) resistance of Ru, Co, and Cu lines vs w.

assuming a constant $R = 0.4$ provides the fairest comparison between the three metals. We use reported liner thicknesses of $t = 0.3$ nm for Ru, $t = 1.0$ nm for Co, and $t = 2.0$ nm for

Cu [16,22,28]. The liner thickness affects the conducting cross-sectional area, which is $(2w - t)\times(w\text{-}2t)$ as seen in Fig. 3(a). Thus, the smaller required t for Ru and Co provide a conductance advantage over Cu for narrow lines.

Figures 3(b) and (c) are plots of the calculated resistivity and resistance vs half-pitch w = 10-50 nm, for polycrystalline Ru, Co, and Cu lines. The resistivity of the Ru interconnect increases from ρ = 9.73 μΩcm at w = 50 nm to ρ = 18.9 μΩcm for w = 10 nm, with a corresponding line resistance increase from 19.8 to 1020 Ω/μm. The corresponding increase for the Co line is from ρ = 10.3 to 32.9 μΩcm, which results in a Co line resistance of 21.6 to 2170 Ω/μm, and for the Cu line from ρ = 4.65 to 22.6 μΩcm, yielding 10.3 to 2090 Ω/μm. Ru has the smallest slope and Cu has the steepest slope in both plots, as expected based on the smallest and largest mean free paths, respectively. This difference is enhanced by the smallest and largest liner thickness for Ru and Cu, respectively. As a consequence, there is a resistivity crossover between Ru and Cu at w = 13 nm [Fig. 3(b)], while the corresponding resistance crossover is at w = 19 nm [Fig. 3(c)]. That is, Ru lines with a half-pitch below 19 nm are expected to conduct better than corresponding Cu lines, while they outperform Cu by approximately a factor of two for w = 10 nm. In contrast, Co exhibits a higher resistivity than both Ru and Cu over the entire plotted w = 10-50 nm range, while the Co line resistance is competitive with that of Ru at w = 50 nm, and with that of Cu at w = 10 nm.

V. Conclusions

Epitaxial Ru(0001) and Co(0001) films were sputtered deposited onto Al_2O_3(0001). Transport measurements with negligible resistance contributions from surface roughness and grain boundary scattering indicate a mean free path λ = 6.7 ± 0.3 nm for Ru and λ = 19.5 ± 1.0 nm for Co. In these epitaxial films, a crossover in resistivity is observed between Ru and Co at a thickness d = 25 nm. The Ru conductance of polycrystalline interconnects in 2:1 aspect ratio trenches is predicted to exceed that of Cu for half-pitch widths w < 19 nm, while the conductance of Co lines becomes comparable to that of Cu at w = 10 nm. These results confirm the promising properties of Ru and Co as potential Cu replacement metals for narrow interconnect lines.

ACKNOWLEDGMENT

The authors acknowledge NSF under grant Nos. 1740271 and 1712752 as well as the NY State Empire State Development's Division of Science, Technology and Innovation (NYSTAR) through Focus Center-NY–RPI Contract C150117.

REFERENCES

[1] S. M. Rossnagel and T. S. Kuan, Alteration of Cu conductivity in the size effect regime, J. Vac. Sci. Technol. B Microelectron. Nanom. Struct. **22**, 240 (2004).

[2] J. S. Chawla, F. Gstrein, K. P. O'Brien, J. S. Clarke, and D. Gall, Electron scattering at surfaces and grain boundaries in Cu thin films and wires, Phys. Rev. B **84**, 235423 (2011).

[3] J. S. Chawla and D. Gall, Specular electron scattering at single-crystal Cu(001) surfaces, Appl. Phys. Lett. **94**, 252101 (2009).

[4] P. Y. Zheng, R. P. Deng, and D. Gall, Ni doping on Cu surfaces: Reduced copper resistivity, Appl. Phys. Lett. **105**, 131603 (2014).

[5] P. Zheng, T. Zhou, and D. Gall, Electron channeling in TiO 2 coated Cu layers, Semicond. Sci. Technol. **31**, 055005 (2016).

[6] M. César, D. Liu, D. Gall, and H. Guo, Calculated Resistances of Single Grain Boundaries in Copper, Phys. Rev. Appl. **2**, 044007 (2014).

[7] M. César, D. Gall, and H. Guo, Reducing Grain-Boundary Resistivity of Copper Nanowires by Doping, Phys. Rev. Appl. **5**, 054018 (2016).

[8] D. Choi, X. Liu, P. K. Schelling, K. R. Coffey, and K. Barmak, Failure of semiclassical models to describe resistivity of nanometric, polycrystalline tungsten films, J. Appl. Phys. **115**, 104308 (2014).

[9] T.-H. Kim, et al, Large Discrete Resistance Jump at Grain Boundary in Copper Nanowire, Nano Lett. **10**, 3096 (2010).

[10] J. M. Rickman and K. Barmak, Simulation of electrical conduction in thin polycrystalline metallic films: Impact of microstructure, J. Appl. Phys. **114**, 133703 (2013).

[11] N. A. Lanzillo, et al, Defect and grain boundary scattering in tungsten: A combined theoretical and experimental study, J. Appl. Phys. **123**, 154303 (2018).

[12] Y. Namba, Resistivity and Temperature Coefficient of Thin Metal Films with Rough Surface, Jpn. J. Appl. Phys. **9**, 1326 (1970).

[13] Y. Ke, F. Zahid, V. Timoshevskii, K. Xia, D. Gall, and H. Guo, Resistivity of thin Cu films with surface roughness, Phys. Rev. B **79**, 155406 (2009).

[14] P. Y. Zheng, T. Zhou, B. J. Engler, J. S. Chawla, R. Hull, and D. Gall, Surface roughness dependence of the electrical resistivity of W(001) layers, J. Appl. Phys. **122**, 095304 (2017).

[15] T. Zhou, P. Zheng, S. C. Pandey, R. Sundararaman, and D. Gall, The electrical resistivity of rough thin films: A model based on electron reflection at discrete step edges, J. Appl. Phys. **123**, 155107 (2018).

[16] M. H. van der Veen, et al, Barrier/liner stacks for scaling the Cu interconnect metallization, in *2016 IEEE Int. Interconnect Technol. Conf. / Adv. Met. Conf.* (IEEE, 2016), pp. 28–30.

[17] F. Zahid, Y. Ke, D. Gall, and H. Guo, Resistivity of thin Cu films coated with Ta, Ti, Ru, Al, and Pd barrier layers from first principles, Phys. Rev. B **81**, 045406 (2010).

[18] Xunyuan Zhang, et al, Ruthenium interconnect resistivity and reliability at 48 nm pitch, in *2016 IEEE Int. Interconnect Technol. Conf. / Adv. Met. Conf.* (IEEE, 2016), pp. 31–33.

[19] J. Kelly, et al, Experimental study of nanoscale Co damascene BEOL interconnect structures, in *2016 IEEE Int. Interconnect Technol. Conf. / Adv. Met. Conf.* (IEEE, 2016), pp. 40–42.

[20] V. Kamineni, et al, Tungsten and cobalt metallization: A material study for MOL local interconnects, in *2016 IEEE Int. Interconnect Technol. Conf. / Adv. Met. Conf.* (IEEE, 2016), pp. 105–107.

[21] D. Choi, et al, Electron mean free path of tungsten and the electrical resistivity of epitaxial (110) tungsten films, Phys. Rev. B **86**, 045432 (2012).

[22] Liang Gong Wen, et al, Ruthenium metallization for advanced interconnects, in *2016 IEEE Int. Interconnect Technol. Conf. / Adv. Met. Conf.* (IEEE, 2016), pp. 34–36.

[23] S. Dutta, K. Moors, M. Vandemaele, and C. Adelmann, Finite Size Effects in Highly Scaled Ruthenium Interconnects., IEEE Electron Device Lett. **39**, 268 (2018).

[24] S. Dutta, et al, Thickness dependence of the resistivity of platinum-group metal thin films, J. Appl. Phys. **122**, 025107 (2017).

[25] S. Dutta, et al, Ruthenium interconnects with 58 nm 2 cross-section area using a metal-spacer process, in *2017 IEEE Int. Interconnect Technol. Conf.* (IEEE, 2017).

[26] E. Milosevic, S. Kerdsongpanya, A. Zangiabadi, K. Barmak, and D. Gall, Resistivity Size Effect in Epitaxial Ru(0001) Layers, J. Appl. Phys. **124**, 165105 (2018).

[27] D. Gall, Electron mean free path in elemental metals, J. Appl. Phys. **119**, 085101 (2016).

[28] S. Dutta, et al, Sub-100 nm 2 Cobalt Interconnects, IEEE Electron Device Lett. **39**, 1 (2018).

[29] C. Auth, et al, A 10nm high performance and low-power CMOS technology featuring 3 rd generation FinFET transistors, Self-

Aligned Quad Patterning, contact over active gate and cobalt local interconnects, in *2017 IEEE Int. Electron Devices Meet.* (IEEE, 2017), p. 29.1.1-29.1.4.

[30] A. Yeoh, et al, Interconnect Stack using Self-Aligned Quad and Double Patterning for 10nm High Volume Manufacturing, in *2018 IEEE Int. Interconnect Technol. Conf.* (IEEE, 2018), pp. 144–147.

[31] K. Fuchs and N. F. Mott, The conductivity of thin metallic films according to the electron theory of metals, Math. Proc. Cambridge Philos. Soc. **34**, 100 (1938).

[32] E. H. Sondheimer, The mean free path of electrons in metals, Adv. Phys. **1**, 1 (1952).

[33] A. F. Mayadas and M. Shatzkes, Electrical-Resistivity Model for Polycrystalline Films: the Case of Arbitrary Reflection at External Surfaces, Phys. Rev. B **1**, 1382 (1970).

[34] J. Brandenburg, R. Hühne, L. Schultz, and V. Neu, Domain structure of epitaxial Co films with perpendicular anisotropy, Phys. Rev. B **79**, 054429 (2009).

[35] W. M. Yim and R. J. Paff, Thermal expansion of AlN, sapphire, and silicon, J. Appl. Phys. **45**, 1456 (1974).

[36] D. Zhang, Electronic structure and properties of pure cobalt, Sci. China, Chinese Acad. Sci. Technol. Sci. **42**, 3705 (1994).

[37] A. S. Ingason, F. Magnus, S. Olafsson, and J. T. Gudmundsson, Morphology of TiN thin films grown on MgO(001) by reactive dc magnetron sputtering, J. Vac. Sci. Technol. A Vacuum, Surfaces, Film. **28**, 912 (2010).

[38] P. Zheng, B. D. Ozsdolay, and D. Gall, Epitaxial growth of tungsten layers on MgO (001), J. Vac. Sci. Technol. A Vacuum, Surfaces, Film. **33**, 061505 (2015).

[39] J. M. Purswani, T. Spila, and D. Gall, Growth of epitaxial Cu on MgO(001) by magnetron sputter deposition, Thin Solid Films **515**, 1166 (2006).

[40] R. W. Powell, R. P. Tye, and M. J. Woodman, The thermal conductivity and electrical resistivity of polycrystalline metals of the platinum group and of single crystals of ruthenium, J. Less Common Met. **12**, 1 (1967).

[41] H. Masumoto, H. Saito, and M. Kikuchi, Magneto-Resistance Effect and Electric Resistance of Single Crystals of Cobalt, Sci. Reports Res. Institutes Tohoku Univ. Ser. A-Physics Chem. Metall. **S 18**, 84 (1966).

[42] T. Zhou and D. Gall, Resistivity scaling due to electron surface scattering in thin metal layers, Phys. Rev. B **97**, 165406 (2018).

[43] Y. P. Timalsina, et al, Evidence of enhanced electron-phonon coupling in ultrathin epitaxial copper films, Appl. Phys. Lett. **103**, 191602 (2013).

[44] J. S. Chawla, X. Y. Zhang, and D. Gall, Epitaxial TiN(001) wetting layer for growth of thin single-crystal Cu(001), J. Appl. Phys. **110**, 043714 (2011).

[45] J. S. Chawla and D. Gall, Epitaxial Ag(001) grown on MgO(001) and TiN(001): Twinning, surface morphology, and electron surface scattering, J. Appl. Phys. **111**, 043708 (2012).

[46] D. Gall, Metals for low-resistivity interconnects, 2018 IEEE Int. Interconnect Technol. Conf. 157 (2018).

[47] E. Milosevic, et al, Validity and Application of the TCR Method to MOL Contacts, in *2018 IEEE Int. Interconnect Technol. Conf. / Adv. Met. Conf.* (IEEE, 2018), pp. 36–38.

[48] H. Huang, et al, Impact of liner metals on copper resistivity at beyond 7nm dimensions, 2018 IEEE Int. Interconnect Technol. Conf. / Adv. Met. Conf. 13 (2018).

[49] J. M. Purswani and D. Gall, Electron scattering at single crystal Cu surfaces, Thin Solid Films **516**, 465 (2007).

[50] J. S. Chawla, F. Zahid, H. Guo, and D. Gall, Effect of O2 adsorption on electron scattering at Cu(001) surfaces, Appl. Phys. Lett. **97**, 132106 (2010).

[51] Savornin, Contribution a l'etude des proprietes electriques et, Ann. Phys. (Paris). **13**, 1355 (1960).

[52] A. K. Pal, S. Chaudhari, and A. K. Barua, Electrical resistivity and temperature coefficient of Cobalt films, J. Appl. Phys. D - Appl. Phys. **9**, 2261 (1976).

[53] Y. F. Zhu, X. Y. Lang, W. T. Zheng, and Q. Jiang, Electron Scattering and Electrical Conductance in Polycrystalline Metallic Films and Wires: Impact of Grain Boundary Scattering Related to Melting Point, ACS Nano **4**, 3781 (2010).

[54] K. Gregorczyk, P. Banerjee, and G. W. Rubloff, Conduction in ultrathin ruthenium electrodes prepared by atomic layer deposition, Mater. Lett. **73**, 43 (2012).

[55] H. Li, D. B. Farmer, R. G. Gordon, Y. Lin, and J. Vlassak, Vapor Deposition of Ruthenium from an Amidinate Precursor, J. Electrochem. Soc. **154**, D642 (2007).

[56] G. J. Vangurp, Resistivity, grain size and structure of vacuum deposited Co films, J. Appl. Phys. **46**, 1922 (1975).

[57] E. E. Mola and L. Plata, On the Electrical Resistivity of Evaporated, Surf. Sci. **34**, 561 (1973).

[58] M. Wislicenus, R. Liske, L. Gerlich, B. Vasilev, and A. Preusse, Microelectronic Engineering Cobalt advanced barrier metallization : A resistivity composition analysis, Microelectron. Eng. **137**, 11 (2015).

[59] H.-D. Liu, Y.-P. Zhao, G. Ramanath, S. P. Murarka, and G.-C. Wang, Thickness dependent electrical resistivity of ultrathin (<40 nm) Cu films, Thin Solid Films **384**, 151 (2001).

[60] T. Sun, et al, Surface and grain-boundary scattering in nanometric Cu films, Phys. Rev. B **81**, 155454 (2010).

[61] J.-W. Lim, K. Mimura, and M. Isshiki, Thickness dependence of resistivity for Cu films deposited by ion beam deposition, Appl. Surf. Sci. **217**, 95 (2003).

[62] J. J. Plombon, E. Andideh, V. M. Dubin, and J. Maiz, Influence of phonon, geometry, impurity, and grain size on Copper line resistivity, Appl. Phys. Lett. **89**, 113124 (2006).

[63] W. Steinhögl, G. Schindler, G. Steinlesberger, M. Traving, and M. Engelhardt, Comprehensive study of the resistivity of copper wires with lateral dimensions of 100 nm and smaller, J. Appl. Phys. **97**, 023706 (2005).

[64] T. Sun, et al, Dominant role of grain boundary scattering in the resistivity of nanometric Cu films, Phys. Rev. B **79**, 041402 (2009).